EURASIP Journal on Applied Signal Processing 2005:6, 972–980

Carrier and Clock Recovery in (Turbo-) Coded Systems: Cramér-Rao Bound and Synchronizer Performance

N. Noels
Department of Telecommunications and Information Processing (TELIN), Ghent University, Sint-Pietersnieuwstraat 41, 9000 Ghent, Belgium
Email: nnoels@telin.ugent.be

H. Steendam
Department of Telecommunications and Information Processing (TELIN), Ghent University, Sint-Pietersnieuwstraat 41, 9000 Ghent, Belgium
Email: hs@telin.ugent.be

M. Moeneclaey
Department of Telecommunications and Information Processing (TELIN), Ghent University, Sint-Pietersnieuwstraat 41, 9000 Ghent, Belgium
Email: mm@telin.ugent.be

Received 30 September 2003; Revised 26 May 2004

In this paper, we derive the Cramér-Rao bound (CRB) for joint carrier phase, carrier frequency, and timing estimation from a noisy linearly modulated signal with *encoded* data symbols. We obtain a closed-form expression for the CRB in terms of the marginal a posteriori probabilities of the coded symbols, allowing efficient numerical evaluation of the CRB for a wide range of coded systems by means of the BCJR algorithm. Simulation results are presented for a rate 1/2 turbo code combined with QPSK mapping. We point out that the synchronization parameters for the coded system are essentially decoupled. We find that, at the normal (i.e., low) operating SNR of the turbo-coded system, the *true* CRB for *coded* transmission is (i) essentially the same as the *modified* CRB and (ii) considerably smaller than the *true* CRB for *uncoded* transmission. Comparison of actual synchronizer performance with the CRB for turbo-coded QPSK reveals that a "code-aware" soft-decision-directed *synchronizer* can perform very closely to this CRB, whereas "code-unaware" estimators such as the conventional *non-data-aided* algorithm are substantially worse; when operating on coded signals, the performance of the latter synchronizers is still limited by the CRB for uncoded transmission.

Keywords and phrases: carrier recovery, clock recovery, coded systems, Cramér-Rao bound, synchronizer performance.

1. INTRODUCTION

The impressive performance of turbo receivers implicitly assumes perfect synchronization, that is, the carrier phase, frequency offset, and time delay must be recovered accurately before data detection. Synchronization for turbo-encoded systems is yet a very challenging task since the receiver usually operates at extremely low SNR values. The development of accurate synchronization techniques has therefore recently received a lot of attention in the technical literature.

A common approach to judge the performance of parameter estimators is to compare their resulting mean square error (MSE) with the Cramér-Rao bound (CRB), which is a fundamental lower bound on the error variance of unbiased estimators [1]. In order to avoid the computational complexity related to the *true* CRB, a *modified* CRB (MCRB) has been derived in [2, 3]. The MCRB is much simpler to evaluate than the CRB but is, in general, looser (i.e., lower) than the CRB, especially at low SNR. In [4, 5, 6, 7], the CRB for the estimation of carrier phase, carrier frequency, and timing delay from *uncoded* data symbols has been obtained and discussed. In [8], the CRB for carrier phase estimation from *coded* data has been expressed in terms of the marginal a posteriori probabilities (APPs) of the coded symbols.

In this contribution, we derive the CRB for *joint* carrier phase, carrier frequency offset, and timing recovery in *coded* systems. Again we obtain a closed-form expression for the CRB in terms of the marginal APPs, allowing the numerical evaluation of the bound for a wide range of coded systems, including schemes with iterative detection (turbo schemes). This CRB is evaluated for rate 1/2 turbo-coded QPSK, and compared to (i) the MCRB, (ii) the CRB for uncoded

transmission, and (iii) the MSE of some practical synchronizers. Our results point out that, at the normal operating SNR of the turbo code, (i) the CRB is essentially the same as the MCRB, (ii) the CRB is significantly smaller than the CRB for uncoded transmission, and (iii) the CRB is a tight lower bound on the MSE resulting from the joint synchronization and turbo-decoding scheme the authors proposed in [9].

2. PROBLEM FORMULATION

Consider an observation vector $\mathbf{r}$ with a probability density function $p(\mathbf{r};\mathbf{u})$ that depends on a deterministic vector parameter $\mathbf{u}$. Suppose that from the observation $\mathbf{r}$, one is able to produce an *unbiased* estimate $\hat{\mathbf{u}}$ of the parameter $\mathbf{u}$, that is, $E_{\mathbf{r}}[\hat{\mathbf{u}}] = \mathbf{u}$ for all $\mathbf{u}$; the expectation $E_{\mathbf{r}}[\cdot]$ is with respect to $p(\mathbf{r};\mathbf{u})$. Then the estimation error variance is lower bounded by the CRB [1]: $E_{\mathbf{r}}[(\hat{u}_i - u_i)^2] \geq \mathrm{CRB}_i(\mathbf{u})$, where $\mathrm{CRB}_i(\mathbf{u})$ is the ith diagonal element of the inverse of the *Fisher information matrix* (FIM) $\mathbf{J}(\mathbf{u})$. The (i, j)th element of $\mathbf{J}(\mathbf{u})$ is given by

$$\begin{aligned}\mathbf{J}_{i,j}(\mathbf{u}) &= E_{\mathbf{r}}\left[-\frac{\partial^2}{\partial u_i \partial u_j}\ln\left(p(\mathbf{r};\mathbf{u})\right)\right] \\ &= E_{\mathbf{r}}\left[\frac{\partial}{\partial u_i}\ln\left(p(\mathbf{r};\mathbf{u})\right)\frac{\partial}{\partial u_j}\ln\left(p(\mathbf{r};\mathbf{u})\right)\right].\end{aligned} \tag{1}$$

The probability density $p(\mathbf{r};\mathbf{u})$ of $\mathbf{r}$, corresponding to a given value of $\mathbf{u}$, is called the *likelihood function* of $\mathbf{u}$, while $\ln(p(\mathbf{r};\mathbf{u}))$ is the *log-likelihood function* of $\mathbf{u}$. Note that $\mathbf{J}(\mathbf{u})$ is a symmetrical matrix. When the element $\mathbf{J}_{i,j}(\mathbf{u}) = 0$, the parameters u_i and u_j are said to be *decoupled*.

When the observation $\mathbf{r}$ depends not only on the parameter $\mathbf{u}$ to be estimated but also on a nuisance vector parameter $\mathbf{v}$, the likelihood function of $\mathbf{u}$ is obtained by averaging the likelihood function $p(\mathbf{r}|\mathbf{v};\mathbf{u})$ of the vector $(\mathbf{u},\mathbf{v})$ over the a priori distribution of the nuisance parameter: $p(\mathbf{r};\mathbf{u}) = E_{\mathbf{v}}[p(\mathbf{r}|\mathbf{v};\mathbf{u})]$. We refer to $p(\mathbf{r}|\mathbf{v};\mathbf{u})$ as the *joint* likelihood function, as $p(\mathbf{r}|\mathbf{v};\mathbf{u})$ is relevant to the joint estimation of $\mathbf{u}$ and $\mathbf{v}$.

We consider the complex baseband representation $r(t)$ of a noisy linearly modulated signal:

$$r(t) = \sum_{k=-K}^{K} a_k h(t - kT - \tau)\exp\left(j(\theta + 2\pi F t)\right) + w(t), \tag{2}$$

where $\mathbf{a} = (a_{-K}, \ldots, a_K)$ is a vector of $L = 2K + 1$ symbols taken from an M-PSK, M-QAM, or M-PAM constellation according to a combination of an encoding rule and a mapping rule; $h(t)$ is an even, *real-valued* unit-energy square-root Nyquist pulse; τ is the time delay; θ is the carrier phase at $t = 0$; F is the carrier frequency offset; T is the symbol interval; $w(t)$ is complex-valued zero-mean Gaussian noise with independent real and imaginary parts, each having a normalized power spectral density of $N_0/(2E_s)$, with E_s and N_0 denoting the symbol energy and the noise power spectral density, respectively.

With $\mathbf{u} = (u_1, u_2, u_3) = (\theta, F, \tau)$ and $\mathbf{v} = \mathbf{a}$, the joint likelihood function $p(\mathbf{r}|\mathbf{v};\mathbf{u})$ resulting from (2) is Gaussian, with a mean depending on $(\mathbf{u},\mathbf{v})$ and a covariance matrix that is independent of $(\mathbf{u},\mathbf{v})$. Within a factor not depending on $(\mathbf{u},\mathbf{v})$, $p(\mathbf{r}|\mathbf{v};\mathbf{u})$ is given by

$$p(\mathbf{r}|\mathbf{v};\mathbf{u}) = p(\mathbf{r}|\mathbf{a};\theta,F,\tau) = \prod_{k=-K}^{K} F\left(a_k, \tilde{z}_k(\theta,F,\tau)\right), \tag{3}$$

where

$$F\left(a_k, \tilde{z}_k(\theta,F,\tau)\right) = \exp\left(\frac{E_s}{N_0}\left(2\,\mathrm{Re}\left[a_k^* \tilde{z}_k(\theta,F,\tau)\right] - |a_k|^2\right)\right). \tag{4}$$

In (3), $\mathbf{r}$ is a vector representation of the signal $r(t)$ from (2), and $\tilde{z}_k(\theta,F,\tau) = z_k(F,\tau)e^{-j\theta}$, where $z_k(F,\tau)$ is defined as

$$z_k(F,\tau) = \int e^{-j2\pi F t} r(t) h(t - kT - \tau)\,dt. \tag{5}$$

Note that $\tilde{z}_k(\theta,F,\tau)$ is obtained by first frequency-correcting $r(t)$ by an amount $-F$, then applying the result to a filter that is matched to the transmit pulse $h(t)$ and sampling the matched filter output at instant $kT + \tau$, and finally rotating the resulting sample over an angle $-\theta$. Hence, $\tilde{z}_k$ is a function of (θ,F,τ), whereas z_k depends only on (F,τ). The log-likelihood function $\ln(p(\mathbf{r};\mathbf{u}))$ resulting from (3) is given by

$$\begin{aligned}\ln p(\mathbf{r};\mathbf{u}) &= \ln p(\mathbf{r};\theta,F,\tau) \\ &= \ln\left(E_{\mathbf{a}}\left[\prod_{k=-K}^{K} F\left(a_k, \tilde{z}_k(\theta,F,\tau)\right)\right]\right).\end{aligned} \tag{6}$$

The expectation $E_{\mathbf{a}}[\cdot]$ in (6) is with respect to the a priori distribution $p(\mathbf{a})$ of the transmitted data sequence $\mathbf{a}$. Computation of the CRB requires the substitution of (6) into (1), and the evaluation of the various expectations included in (6) and (1).

The evaluation of the expectations involved in $\mathbf{J}(\theta,F,\tau)$ and $p(\mathbf{r};\theta,F,\tau)$ is quite tedious. In order to avoid the computational complexity caused by the nuisance parameters, a simpler lower bound, called the modified CRB (MCRB), has been derived in [2, 3], that is, $E_{\mathbf{r}}[(\hat{u}_i - u_i)^2] \geq \mathrm{CRB}_i(\mathbf{u}) \geq \mathrm{MCRB}_i(\mathbf{u})$, where $\mathrm{MCRB}_i(\mathbf{u})$ is the ith diagonal element of the inverse of the *modified* Fisher information matrix (MFIM) $\mathbf{J}^M(\mathbf{u})$. The (i, j)th element of $\mathbf{J}^M(\mathbf{u})$ is given by

$$\begin{aligned}\mathbf{J}^M_{i,j}(\mathbf{u}) &= E_{\mathbf{r},\mathbf{v}}\left[-\frac{\partial^2}{\partial u_i \partial u_j}\ln\left(p(\mathbf{r}|\mathbf{v};\mathbf{u})\right)\right] \\ &= E_{\mathbf{r},\mathbf{v}}\left[\frac{\partial}{\partial u_i}\ln\left(p(\mathbf{r}|\mathbf{v};\mathbf{u})\right)\frac{\partial}{\partial u_j}\ln\left(p(\mathbf{r}|\mathbf{v};\mathbf{u})\right)\right]\end{aligned} \tag{7}$$

and $E_{\mathbf{r},\mathbf{v}}[\cdot]$ denotes averaging over both $\mathbf{r}$ and $\mathbf{v}$, that is, with respect to $p(\mathbf{r},\mathbf{v};\mathbf{u}) = p(\mathbf{r}|\mathbf{v};\mathbf{u})p(\mathbf{v})$. When $p(\mathbf{r}|\mathbf{v};\mathbf{u})$ is Gaussian, (7) is much simpler than (1) as far as analytical evaluation is concerned, because the tedious computation of $p(\mathbf{r};\mathbf{u})$ is avoided.

The MCRB for joint carrier phase, carrier frequency offset, and timing estimation, corresponding to $r(t)$ from (1), is given by [2, 3]

$$E\left[(\hat{\theta}-\theta)^2\right] \geq \mathrm{MCRB}_\theta = \frac{N_0}{2E_sL}, \tag{8}$$

$$E\left[(\hat{F}-F)^2 \cdot T^2\right] \geq \mathrm{MCRB}_F = \frac{3N_0}{2\pi^2E_sL(L^2-1)}, \tag{9}$$

$$E\left[(\hat{\tau}-\tau)^2/T^2\right] \geq \mathrm{MCRB}_\tau = \frac{N_0}{2E_sLT^2\int\left(\dot{h}(t)\right)^2dt}, \tag{10}$$

where $\dot{h}(t) = dh(t)/dt$ and $L = 2K+1$ denotes the number of symbols transmitted within the observation interval. Note that in (9) and (10), the frequency and timing errors have been normalized by the symbol interval T. The MCRB does not depend on the symbol constellation; the shape of the transmit pulse $h(t)$ affects only the quantity $\int(\dot{h}(t))^2dt$ in (10), which is an increasing function of the excess bandwidth of the transmit pulse $h(t)$. The MCRB for phase and timing estimation is inversely proportional to L; the MCRB for frequency estimation is, for large L, inversely proportional to L^3. In [10], the high-SNR limit of the true CRB related to the estimation of a scalar parameter has been evaluated analytically and has been shown to coincide with the MCRB from (8), (9), and (10).

In the next section, we derive a closed-form expression of the CRB resulting from (1) in terms of the marginal APPs of the coded symbols, allowing efficient numerical evaluation of the CRB.

3. DERIVATION OF THE CRB

The log-likelihood function $\ln(p(\mathbf{r};\theta,F,\tau))$ from (6) can be written as

$$\ln p(\mathbf{r};\theta,F,\tau) = \ln\left(\sum_{i=0}^{M^L-1}\Pr\left[\mathbf{a}=\mathbf{c}_i\right]p(\mathbf{r}|\mathbf{c}_i;\theta,F,\tau)\right), \tag{11}$$

where $p(\mathbf{r}|\mathbf{c}_i;\theta,F,\tau)$ is given by (3) and i enumerates all M^L symbol sequences $\mathbf{c}_i$ of length L. Denoting by ξ the set of legitimate coded sequences of length L, we have $\Pr[\mathbf{a}=\mathbf{c}_i] = M^{-\rho L}$ for $\mathbf{c}_i \in \xi$ and $\Pr[\mathbf{a}=\mathbf{c}_i] = 0$ otherwise, with ρ and M denoting the rate of the code and the number of constellation points, respectively. Differentiation of (11) yields

$$\frac{\partial}{\partial u_\ell}\ln\left(p(\mathbf{r};\mathbf{u})\right) = \sum_{i=0}^{M^L-1}\frac{\Pr\left[\mathbf{a}=\mathbf{c}_i\right]p(\mathbf{r}|\mathbf{c}_i;\theta,F,\tau)}{p(\mathbf{r};\theta,F,\tau)}\frac{\partial}{\partial u_\ell}\ln\left(p(\mathbf{r}|\mathbf{c}_i;\mathbf{u})\right). \tag{12}$$

Making use of Bayes' rule, we obtain

$$\frac{\Pr\left[\mathbf{a}=\mathbf{c}_i\right]p(\mathbf{r}|\mathbf{c}_i;\theta,F,\tau)}{p(\mathbf{r};\theta,F,\tau)} = \Pr\left[\mathbf{a}=\mathbf{c}_i|\mathbf{r};\theta,F,\tau\right], \tag{13}$$

where $\Pr[\mathbf{a}=\mathbf{c}_i|\mathbf{r};\theta,F,\tau]$ $(i=0,\ldots,M^L-1)$ are the *joint* symbol a posteriori probabilities (APPs); note from (3) that $\Pr[\mathbf{a}=\mathbf{c}_i|\mathbf{r};\theta,F,\tau]$ is a function of $\mathbf{c}_i$ and $\tilde{\mathbf{z}} = (\tilde{z}_{-K},\ldots,\tilde{z}_K)^T$ only. Using (13) and (3), (12) is transformed into

$$\frac{\partial}{\partial u_\ell}\ln\left(p(\mathbf{r};\mathbf{u})\right) = 2\frac{E_s}{N_0}\sum_{k=-K}^{K}\mathrm{Re}\left(\mu_k^*(\tilde{\mathbf{z}})\tilde{z}_{\ell,k}\right), \tag{14}$$

where the subscript ℓ denotes differentiation with respect to u_ℓ, that is,

$$\tilde{z}_{\ell,k} = \frac{\partial}{\partial u_\ell}(\tilde{z}_k) \tag{15}$$

and $\mu_k(\tilde{\mathbf{z}})$ is the a posteriori average of the symbol a_k:

$$\begin{aligned}\mu_k(\tilde{\mathbf{z}}) &= \sum_{i=0}^{M^L-1}(\mathbf{c}_i)_k\Pr\left[\mathbf{a}=\mathbf{c}_i|\mathbf{r};\theta,F,\tau\right]\\ &= \sum_{m=0}^{M-1}\alpha_m\Pr\left[a_k=\alpha_m|\mathbf{r};\theta,F,\tau\right].\end{aligned} \tag{16}$$

In (16), $(\mathbf{c}_i)_k$ is the kth component of the vector $\mathbf{c}_i$, $(\alpha_0, \alpha_1,\ldots,\alpha_{M-1})$ denotes the set of constellation points, and $\Pr[a_k=\alpha_m|\mathbf{r};\theta,F,\tau]$ $(m=0,\ldots,M-1)$ are the *marginal* symbol APPs. We emphasize that no approximation is involved when arriving at (16). The second line of (16) simply expresses the a posteriori average of a_k in terms of the marginal APP of a_k, rather than the joint APP of $(a_{-K},\ldots,a_K)$.

Substitution of (14) into (1) yields an exact expression of the FIM in terms of the a posteriori symbol averages $\mu_k(\tilde{\mathbf{z}})$, which in turn depend on the marginal symbol APPs $\Pr[a_k=\alpha_m|\mathbf{r};\theta,F,\tau]$. One obtains

$$\mathbf{J}_{i,j} = 4\left(\frac{E_s}{N_0}\right)^2\sum_{k=-K}^{K}\sum_{k'=-K}^{K}E\left[\mathrm{Re}\left[\mu_k^*(\tilde{\mathbf{z}})\tilde{z}_{i,k}\right]\mathrm{Re}\left[\mu_{k'}^*(\tilde{\mathbf{z}})\tilde{z}_{j,k'}\right]\right], \tag{17}$$

where $E[\cdot]$ denotes averaging over the quantities $\tilde{\mathbf{z}}$, $\tilde{z}_{i,k}$, and $\tilde{z}_{j,k'}$. As this averaging cannot be done analytically, we have to resort to a numerical evaluation.

A brute force evaluation of the FIM involves replacing in (17) the statistical average $E[\cdot]$ by an arithmetical average over a large number of realizations of $(\tilde{\mathbf{z}},\tilde{z}_{i,k},\tilde{z}_{j,k'})$ that are computer-generated according to the joint distribution of $(\tilde{\mathbf{z}},\tilde{z}_{i,k},\tilde{z}_{j,k'})$. However, because of the correlation between the quantities $\tilde{\mathbf{z}}$, $\tilde{z}_{i,k}$, and $\tilde{z}_{j,k'}$, a brute force numerical averaging is time consuming. In the appendix, we show how the computational complexity can be reduced by performing the averaging in (17) over $\tilde{\mathbf{z}}$, $\tilde{z}_{i,k}$, and $\tilde{z}_{j,k'}$ in two steps. In the first step, we average over $\tilde{z}_{i,k}$ and $\tilde{z}_{j,k'}$, conditioned on $\tilde{\mathbf{z}}$; this conditional averaging is done *analytically*. In the second step, we remove the conditioning by *numerically* averaging over $\tilde{\mathbf{z}}$; the generation of realizations of $\tilde{\mathbf{z}}$ is easy, as $\tilde{\mathbf{z}} = \mathbf{a}+\mathbf{n}$, where the complex-valued zero-mean Gaussian noise vector $\mathbf{n}$ has statistically independent components with variance N_0/E_s, and the data symbol vector $\mathbf{a}$ results from the encoding and mapping of a randomly generated information bit sequence.

The numerical evaluation of the FIM requires the computation of the a posteriori symbol averages $\mu_k(\tilde{\mathbf{z}})$ that correspond to the realizations of the vector $\tilde{\mathbf{z}}$. These a posteriori symbol averages are given by the second line of (16) in terms of the marginal symbol APPs $\Pr[a_k = \alpha_m|\mathbf{r};\theta,F,\tau]$. In principle, the marginal symbol APPs can be obtained as appropriate summations of joint symbol APPs $\Pr[\mathbf{a} = \mathbf{c}_i|\mathbf{r};\theta,F,\tau]$, which in turn can be computed from (13) and (3). However, the computational complexity of this procedure increases exponentially with the sequence length L.

For codes that are described by means of a trellis, the marginal symbol APPs can be easily computed from the trellis state APPs and state transition APPs, which in turn can be determined efficiently from $\tilde{\mathbf{z}}$ by means of the Bahl-Cocke-Jelinek-Raviv (BCJR) algorithm [11]. As its computational complexity grows only linearly with the number of states and with the sequence length L, the BCJR algorithm is the appropriate tool for marginal symbol APP computation in case of linear block codes, convolutional codes, and trellis codes, provided that the number of states is manageable.

When the coded symbol sequence results from the (serial or parallel) concatenation of two encoders that are separated by an interleaver (such as turbo codes [12]), the underlying overall trellis has a number of states that grow exponentially with the interleaver size. However, when the constituent encoders themselves are described by a small trellis, the state APPs and state transition APPs of the individual trellises can be efficiently computed by means of iterated application of the BCJR algorithm to each of the trellises, with exchange of extrinsic information between the BCJR algorithms at each iteration. When the coded bits (conditioned on $\mathbf{r}$ and (θ,F,τ)) can be considered as independent (which is a reasonable assumption when the interleaver size is large), this iterative procedure yields the correct APPs after convergence [13]. Whereas a turbo decoder makes use of the state APPs and state transition APPs (resulting from iterated application of the BCJR algorithm) to compute the log-likelihood ratios of the information bits, we use these APPs to compute the marginal symbol APPs instead.

Once we have obtained the numerical value of the 3×3 FIM (15), the CRBs related to the joint estimation of (θ,F,τ) are obtained from matrix inversion. However, in many practical situations, a subset of the parameters (θ,F,τ) is estimated, assuming the remaining parameters to be perfectly known; in this case, the relevant FIM is obtained by deleting from the 3×3 FIM (15) the rows and columns that correspond to the parameters that are known. Therefore, we consider the following cases.

(i) The CRB for the estimation of u_i *jointly with* u_j *and* u_k is given by

$$\mathrm{CRB}_i = \frac{\mathbf{J}_{j,j}\mathbf{J}_{k,k} - \mathbf{J}_{j,k}^2}{\mathbf{J}_{i,i}\mathbf{J}_{j,j}\mathbf{J}_{k,k} - \mathbf{J}_{i,i}\mathbf{J}_{j,k}^2 - \mathbf{J}_{j,j}\mathbf{J}_{i,k}^2 - \mathbf{J}_{k,k}\mathbf{J}_{i,j}^2 + 2\mathbf{J}_{i,j}\mathbf{J}_{j,k}\mathbf{J}_{i,k}}. \tag{18}$$

(ii) The CRB for the estimation of u_i *assuming* u_j *and* u_k *to be perfectly known* is given by

$$\mathrm{CRB}_i = \frac{1}{\mathbf{J}_{i,i}}. \tag{19}$$

(iii) The CRB for the estimation of u_i *jointly with* u_j *assuming* u_k *to be perfectly known* is given by

$$\mathrm{CRB}_i = \frac{\mathbf{J}_{j,j}}{\mathbf{J}_{i,i}\mathbf{J}_{j,j} - \mathbf{J}_{i,j}^2}. \tag{20}$$

4. NUMERICAL RESULTS AND DISCUSSION

Simulation results are obtained for the observation of $L = 1001$ QPSK turbo-encoded symbols. The transmit pulse is a square-root cosine rolloff pulse with an excess bandwidth of 20% or 100%. The turbo encoder consists of the parallel concatenation of two identical recursive systematic rate 1/2 convolutional codes with generator polynomials $(37)_8$ and $(21)_8$, through a pseudorandom interleaver of length L; the output of the turbo encoder is punctured to obtain an overall rate of 1/2 and Gray-mapped onto the QPSK constellation.

As far as this simulation setup is concerned, our numerical results indicate that $J_{ij}^2 \ll J_{ii}J_{jj}$ for all $i,j \in \{1,2,3\}$ and $i \neq j$. This implies that both (18) and (20) yield $\mathrm{CRB}_i \cong 1/J_{ii}$. Comparing this result with (19) indicates that the CRB related to the estimation of a synchronization parameter (carrier phase, carrier frequency offset or timing) is essentially independent of the considered scenario (joint estimation of all three parameters, joint estimation of two parameters with the third parameter assumed to be known, estimation of one parameter with the other two parameters assumed to be known). This means that there is almost no coupling between the parameters θ, F, and τ, so that (at least for small errors) the inaccuracy in one of the parameters does not impact the estimation of the other parameters. A similar observation regarding the elements of the FIM for uncoded transmission and the MFIM (7), resulting from $r(t)$ given by (2), has been reported in [7] and [3], respectively.

For the joint estimation of θ, F, and τ, Figure 1 shows the ratio CRB/MCRB (the left ordinate) along with the BER corresponding to perfect synchronization (the right ordinate) as a function of E_s/N_0 per coded symbol (solid lines). The ratio CRB/MCRB for uncoded transmission (UC) is also displayed (dashed lines). We make the following observations.

(i) The ratio CRB/MCRB related to timing estimation increases with decreasing rolloff. The same behavior has been observed in [7], but for uncoded transmission only.

(ii) The ratios CRB/MCRB related to phase estimation and frequency estimation are essentially the same and do not depend on the shape of the transmitted square-root Nyquist pulse $h(t)$. The same behavior has been observed in [4], but for uncoded transmission only.

(iii) We denote by $\mathrm{CRB}_{\mathrm{uncoded}}$ and $\mathrm{CRB}_{\mathrm{coded}}$ the CRBs related to uncoded and coded transmissions, respectively. We observe that $\mathrm{CRB}_{\mathrm{uncoded}} > \mathrm{CRB}_{\mathrm{coded}}$. This implies that it is potentially more accurate to estimate

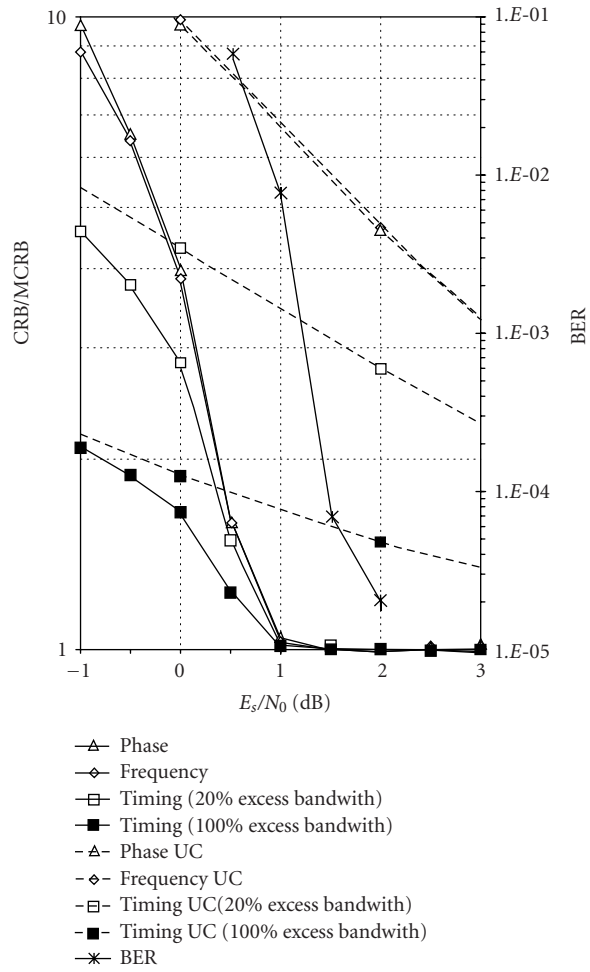

FIGURE 1: Comparison of the ratio CRB/MCRB for turbo-encoded transmission with the ratio CRB/MCRB for uncoded (UC) transmission; for QPSK symbols and an observation length $L = 1001$.

the synchronizer parameters from coded data than from uncoded data.

(iv) We restrict our attention to coded transmission. The MSE resulting from "code-aware" synchronizers (that exploit code properties during the estimation process) is lower bounded by $\mathrm{CRB}_{\mathrm{coded}}$. However, the MSE of synchronizers that do not exploit code properties (i.e., "code-unaware" synchronizers) is lower bounded by $\mathrm{CRB}_{\mathrm{uncoded}}$ (even when operating on coded systems). At the normal operating SNR of the turbo code (this excludes very low SNR at which the turbo code becomes unreliable, as well as very high SNR at which uncoded transmission becomes reliable), $\mathrm{CRB}_{\mathrm{coded}}$ is considerably smaller than $\mathrm{CRB}_{\mathrm{uncoded}}$. It follows that code-aware synchronizers are potentially more accurate than code-unaware synchronizers when operating on coded signals. The ratio $\mathrm{CRB}_{\mathrm{uncoded}}/\mathrm{CRB}_{\mathrm{coded}}$ provides a quantitative indication *to what extent* synchronizer performance can be improved by making clever use of the code structure.

(v) At high SNR, the CRB converges to the MCRB; this behavior is consistent with [10]. When E_s/N_0 decreases, a critical value $(E_s/N_0)_{\mathrm{crit}}$ is reached, below which the CRB starts to diverge from the MCRB. Figure 1 shows that, for coded transmission, this critical value corresponds to a BER between 10^{-2} and 10^{-3} (a similar observation has been reported for uncoded transmission [7, 8]: $(E_s/N_0)_{\mathrm{crit}}$ for uncoded transmission also corresponds to BER $\cong 10^{-3}$, but exceeds $(E_s/N_0)_{\mathrm{crit}}$ for coded transmission by an amount equal to the coding gain). This indicates that, even at the (very low) operating SNR of the coded system, the CRB is very well approximated by the MCRB (which is much simpler to evaluate).

5. ACTUAL ESTIMATOR PERFORMANCE

In this section, we will show that $\mathrm{CRB}_{\mathrm{coded}}$ and $\mathrm{CRB}_{\mathrm{uncoded}}$ are useful benchmarks for the MSE resulting from code-ware and code-unaware synchronizers, respectively. Therefore, we consider practical joint phase and frequency estimators, operating on the rate 1/2 turbo-encoded QPSK signal from the previous section. We assume that the frequency offset does not exceed 10% of the baud rate, that is, $|FT| \leq 0.1$. The MSE for phase and frequency estimation is shown as a function of the SNR in Figures 2 and 3. As the joint estimation of carrier phase and frequency is only marginally affected by a small timing estimation error (because (θ, F) and τ are essentially decoupled), we have determined the mean square phase and frequency error assuming the timing to be known. An observation of $L = 1001$ (i.e., block size of the code) unknown data symbols was considered. A preamble of N known pilot symbols (PS) at the beginning of each block may be used for initialization (to be explained in Sections 5.1 and 5.2). A minimum of 10 000 trials has been run; at each trial, a new phase offset θ and a new frequency offset FT are taken from a uniform distribution over $[-\pi, \pi]$ and $[-0.1, 0.1]$, respectively.

Two algorithms for joint carrier phase and frequency estimation are considered.

(i) The conventional 4th-power non-data-aided (NDA) synchronizer [14, 15] is a code-unaware algorithm for carrier phase and frequency estimation that is very easy to implement. Moreover, this estimator was proposed in [16] for operation on a turbo-coded signal at very low E_s/N_0. In contrast with the MSE of the code-aware estimators, the MSE of code-unaware estimators is lower bounded by the $\mathrm{CRB}_{\mathrm{uncoded}}$ (with $\mathrm{CRB}_{\mathrm{uncoded}} \geq \mathrm{CRB}_{\mathrm{coded}}$). We will show that the MSE of this NDA synchronizer is close to $\mathrm{CRB}_{\mathrm{uncoded}}$, which indicates that this synchronizer is among the best code-unaware estimators.

(ii) The soft-decision-directed (SDD) synchronizer from [9] is a code-aware algorithm that accepts soft information from the turbo decoder (i.e., "turbo synchronization"). As motivated in [9], it involves a practical implementation of the maximum-likelihood (ML)

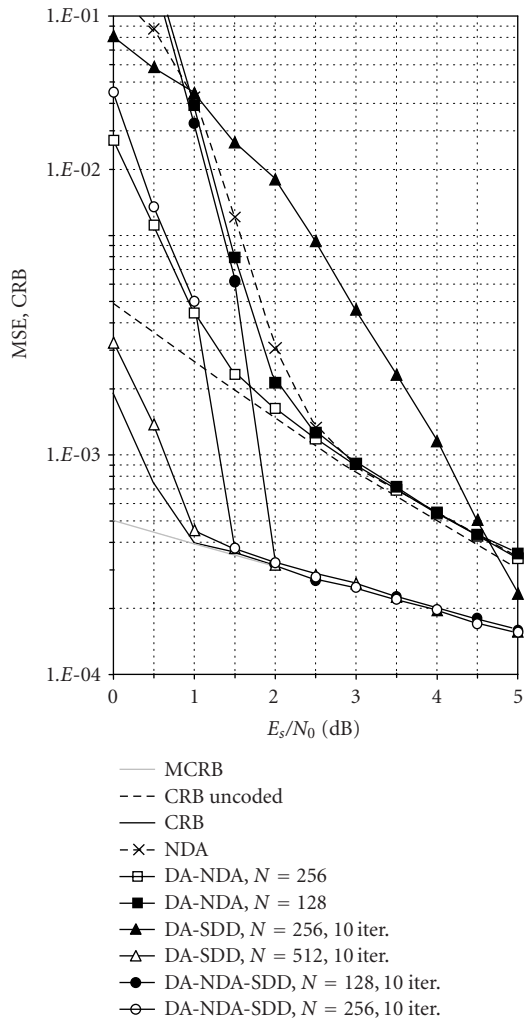

Figure 2: Comparison of the MSE of practical estimators with the CRB (phase estimate).

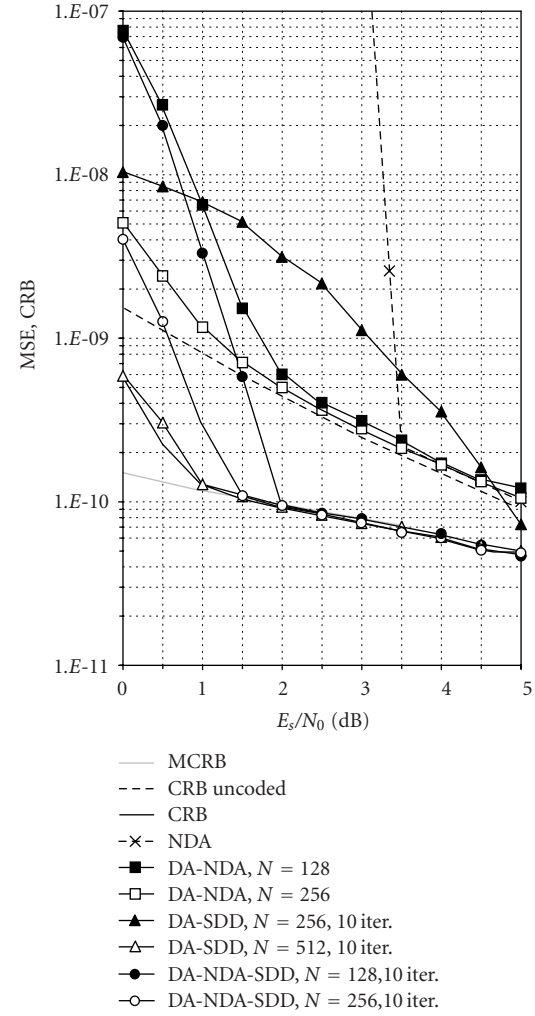

Figure 3: Comparison of the MSE of practical estimators with the CRB (frequency estimate).

estimator by means of the expectation-maximization (EM) algorithm. This iterative algorithm converges to the ML estimate provided that the initial estimate is sufficiently accurate [17]. The ML estimator is known to become asymptotically unbiased and efficient (i.e., the MSE converges to $\mathrm{CRB}_{\mathrm{coded}}$) for an increasing number of observations. Therefore, we expect that the MSE performance of the SDD synchronizer from [9] will closely approach $\mathrm{CRB}_{\mathrm{coded}}$.

The phase error of the turbo synchronizer is measured modulo 2π and supported in the interval $[-\pi, \pi]$. The phase error of the NDA estimator was measured modulo $\pi/2$, that is, in the interval $[-\pi/4, \pi/4]$, as the NDA estimator for QPSK gives a 4-fold phase ambiguity.

5.1. Conventional (code-unaware) NDA estimator

The dashed curve in Figures 2 and 3 corresponds to the MSE for carrier phase and frequency estimation, respectively, as obtained with the (code-unaware) conventional NDA estimator. For $E_s/N_0 \geq 3.5$ dB, the algorithm achieves near-optimal $\mathrm{CRB}_{\mathrm{uncoded}}$ performance. However, for $E_s/N_0 < 3.5$ dB, the performance of the frequency estimator dramatically deteriorates across a narrow SNR interval. This is the so-called *threshold phenomenon*, which is caused by the occurrence of large, spurious frequency errors (outliers) when the SNR drops below a certain threshold and results in a very high frequency error variance at SNR below threshold [14], which also affects the accuracy of the phase estimate.

To show that the $\mathrm{CRB}_{\mathrm{uncoded}}$ can be closely approached by the MSE resulting from code-unaware synchronizers even at low SNR, we replace the conventional NDA frequency estimation with the combined DA and NDA frequency estimation proposed in [18]. This approach consists of a two-stage coarse-fine search. The DA estimator is used to coarsely locate the frequency offset, and then the more accurate NDA estimator attempts to improve the estimate within the residual uncertainty of the coarse estimator. In fact, the search range of the NDA estimator is restricted to the neighborhood of the peak of the DA-based likelihood function. This considerably reduces the probability to estimate an outlier

frequency. As a result, the accuracy below threshold increases dramatically and the MSE approaches the $\mathrm{CRB}_{\mathrm{uncoded}}$. Moreover, the PS can be exploited to resolve the phase ambiguity: after frequency and phase correction, the samples of the preamble are compared to the known pilot symbols and, if necessary, an extra multiple of $\pi/2$ is compensated for. In Figures 2 and 3, the square markers illustrate the MSE for carrier phase and frequency estimation as obtained with this DA-NDA estimator, assuming the initial DA estimate is based on the observation of N preamble symbols. Results are displayed for $N = 128$ and $N = 256$. A threshold is still evident, but the performance below the SNR threshold degrades less rapidly than with the conventional NDA frequency estimator. The more PS are used, the more the threshold softens. Relatively large preambles are required for the DA-NDA estimator to perform closely to the $\mathrm{CRB}_{\mathrm{uncoded}}$, for example, with $N = 256$ the overhead $N/(N + L)$ equals about 20%.

Note that the SNR threshold can also be decreased by increasing the observation length (in [16], $L = 8192$). However, enlarging the observation interval is not always possible. For the sake of completeness, we mention also that a more sophisticated distribution of the PS across the burst may reduce the number of PS required to obtain a certain DA estimation accuracy, thereby increasing the spectral efficiency of the transmission systems [18, 19].

5.2. Soft-decision-directed (code-aware) synchronizer

We consider the (code-aware) SDD synchronizer from [9] and compare its MSE to the new CRB for coded transmission. In our simulations, we used the approximate implementation proposed in [9]: at every turbo decoder iteration, soft decisions on the data symbols are extracted from the decoder and used to update the carrier phase and frequency estimates. This iterative SDD procedure was initialized with a data-aided (DA) frequency and phase estimate obtained from the preamble, or with a combined DA-NDA frequency and phase estimate as described in Section 5.1. We will refer to these synchronization schemes as DA-SDD and DA-NDA-SDD, respectively. The PS are strictly used for the DA initialization, and the (NDA-)SDD algorithm uses only the L coded symbols; therefore the $\mathrm{CRB}_{\mathrm{coded}}$ related to L symbols from Section 3 is the appropriate lower bound on the performance of the SDD algorithms.

Our results indicate the importance of an accurate initial estimate. The curves marked with triangles (circles) in Figures 2 and 3 show the MSE for carrier phase and frequency, respectively, as obtained with the DA-SDD (DA-NDA-SDD) estimator after 10 iterations of the turbo decoder/estimator. With $N = 512$, the DA-SDD estimator performs very closely to the CRB. However, the resulting overhead of about 34% is often not acceptable. Reducing the number of PS to $N = 256$ causes a serious degradation of the DA-SDD estimator. For a given number of PS, the DA-NDA-SDD estimator provides a considerable improvement over the DA-SDD estimator within the useful SNR range of the turbo code and coincides with $\mathrm{CRB}_{\mathrm{coded}}$ at values of SNR larger than about 1.5 dB for $N = 256$ (about 20% overhead) and 2 dB for $N = 128$ (about 11% overhead).

6. CONCLUSION

This contribution derives the CRB for joint carrier phase, carrier frequency offset, and timing estimation from coded signals. The closed-form expression of the CRB in terms of the marginal symbol APPs allows efficient numerical evaluation. It was shown that, at the normal operating SNR of the code (say, $10^{-6} < \mathrm{BER} < 10^{-3}$), the CRB is very close to the MCRB, which in turn is much less than the CRB for uncoded transmission. Furthermore, the CRB for uncoded transmission has been shown to lower bound the MSE of "code-unaware" synchronizers that make no use of the code structure when operating on coded signals. This implies that in order to approach optimal performance, estimators should make clever use of the code properties during the estimation process. The iterative code-aware turbo synchronizer for carrier phase and frequency estimation, presented in [9], has been shown to operate very closely to the CRB for coded transmission, provided that a sufficiently accurate initial estimate is available.

Although using a code-aware synchronizer instead of a code-unaware synchronizer substantially reduces the MSE at the normal operating SNR of the code, it highly depends on the specific coded system considered whether or not this reduction in MSE yields a considerable improvement in BER performance. In [16], code-unaware algorithms for carrier phase, carrier frequency, and timing estimation that operate on a turbo-coded QPSK signal give rise to a BER degradation of only 0.05 dB as compared to a perfectly synchronized system. In this case, there is no need to use code-aware synchronization to further reduce the already very small BER degradation. On the other hand, [20] considers a different turbo-coded QPSK system, where the code-unaware 4th-power NDA phase synchronizer yields a BER degradation of about 1 dB at a BER of 10^{-3}, whereas code-aware phase synchronization reduces this BER degradation to about 0.05 dB only.

No performance results for practical timing estimators have been presented here. However, it has been shown in [21] that applying the turbo synchronization approach to timing estimation from coded signals results in a very low MSEE, which approaches the new CRB for timing estimation from Section 3.

APPENDIX

For further use, we introduce the functions $g(t)$ and $f(t)$ given by

$$g(t) = \int_{-\infty}^{+\infty} h(v)h(t+v)dv, \tag{A.1}$$

$$f(t) = \int u^2 h(u)h(t+u)du \tag{A.2}$$

and denote the first and second derivates of $g(t)$ with respect to t as $\dot{g}(t)$ and $\ddot{g}(t)$, respectively. Note that $g(t)$ is a Nyquist pulse: $g(kT) = \delta_k$. The pulses $g(t)$ and $\ddot{g}(t)$ are even in t, whereas $\dot{g}(t)$ is an odd function of t. For even $h(t)$, the function $f(t)$ is also even in t.

It follows from (17) that $\mathbf{J}_{i,j}$ can be expressed in terms of the following expectations:

$$E[\mu_k^*(\tilde{\mathbf{z}})\mu_{k'}^*(\tilde{\mathbf{z}})\tilde{z}_{i,k}\tilde{z}_{j,k'}] = E_{\tilde{\mathbf{z}}}[\mu_k^*(\tilde{\mathbf{z}})\mu_{k'}^*(\tilde{\mathbf{z}})E[\tilde{z}_{i,k}\tilde{z}_{j,k'}|\tilde{\mathbf{z}}]],$$
$$E[\mu_k^*(\tilde{\mathbf{z}})\mu_{k'}(\tilde{\mathbf{z}})\tilde{z}_{i,k}\tilde{z}_{j,k'}^*] = E_{\tilde{\mathbf{z}}}[\mu_k^*(\tilde{\mathbf{z}})\mu_{k'}(\tilde{\mathbf{z}})E[\tilde{z}_{i,k}\tilde{z}_{j,k'}^*|\tilde{\mathbf{z}}]], \tag{A.3}$$

where $E_{\tilde{\mathbf{z}}}[\cdot]$ denotes averaging with respect to $\tilde{\mathbf{z}}$. The conditional expectations $E[z_{i,k}z_{j,k'}|\tilde{\mathbf{z}}]$ and $E[z_{i,k}z_{j,k'}^*|\tilde{\mathbf{z}}]$ can be determined analytically. One obtains

$$E[\tilde{z}_{\theta,k}\tilde{z}_{\theta,k'}|\tilde{\mathbf{z}}] = -\tilde{z}_k\tilde{z}_{k'}, \tag{A.4}$$
$$E[\tilde{z}_{\theta,k}\tilde{z}_{\theta,k'}^*|\tilde{\mathbf{z}}] = \tilde{z}_k\tilde{z}_{k'}, \tag{A.5}$$
$$E[\tilde{z}_{\theta,k}\tilde{z}_{F,k'}|\tilde{\mathbf{z}}] = 2\pi(k'T+\tau)\tilde{z}_k\tilde{z}_{k'}, \tag{A.6}$$
$$E[\tilde{z}_{\theta,k}\tilde{z}_{F,k'}^*|\tilde{\mathbf{z}}] = 2\pi(k'T+\tau)\tilde{z}_k\tilde{z}_{k'}^*, \tag{A.7}$$
$$E[\tilde{z}_{\theta,k}\tilde{z}_{\tau,k'}|\tilde{\mathbf{z}}] = -j\tilde{z}_k\sum_{m=-K}^{K}\tilde{z}_m\dot{g}(k'T-mT), \tag{A.8}$$
$$E[\tilde{z}_{\theta,k}\tilde{z}_{\tau,k'}^*|\tilde{\mathbf{z}}] = -j\tilde{z}_k\sum_{m=-K}^{K}\tilde{z}_m^*\dot{g}(k'T-mT), \tag{A.9}$$
$$E[\tilde{z}_{F,k}\tilde{z}_{F,k'}|\tilde{\mathbf{z}}] = -4\pi^2\tilde{z}_k\tilde{z}_{k'}(kT+\tau)(k'T+\tau), \tag{A.10}$$
$$E[\tilde{z}_{F,k}\tilde{z}_{F,k'}^*|\tilde{\mathbf{z}}] = 4\pi^2\tilde{z}_k\tilde{z}_{k'}^*(kT+\tau)(k'T+\tau) + 4\pi^2\frac{N_0}{E_s}f(kT-k'T), \tag{A.11}$$
$$E[\tilde{z}_{F,k}\tilde{z}_{\tau,k'}|\tilde{\mathbf{z}}] = -j2\pi(kT+\tau)\tilde{z}_k\sum_{m=-K}^{K}\tilde{z}_m\dot{g}(k'T-mT), \tag{A.12}$$
$$E[\tilde{z}_{F,k}\tilde{z}_{\tau,k'}^*|\tilde{\mathbf{z}}] = -j2\pi(kT+\tau)\tilde{z}_k\sum_{m=-K}^{K}\tilde{z}_m^*\dot{g}(k'T-mT) + j2\pi\frac{N_0}{E_s}\left\{-\frac{(kT-k'T)}{2}\dot{g}(kT-k'T) - \frac{1}{2}\delta_{k-k'}\right\}, \tag{A.13}$$
$$E[\tilde{z}_{\tau,k}\tilde{z}_{\tau,k'}|\tilde{\mathbf{z}}] = \sum_{m,n=-K}^{K}\tilde{z}_m\tilde{z}_n\dot{g}(kT-mT)\dot{g}(k'T-nT), \tag{A.14}$$
$$E[\tilde{z}_{\tau,k}\tilde{z}_{\tau,k'}^*|\tilde{\mathbf{z}}] = \sum_{m,n=-K}^{K}\tilde{z}_m\tilde{z}_n^*\dot{g}(kT-mT)\dot{g}(k'T-nT) + \frac{N_0}{E_s}(-\ddot{g}(kT-k'T)) - \frac{N_0}{E_s}\sum_{m=-K}^{K}\dot{g}(kT-mT)\dot{g}(k'T-mT). \tag{A.15}$$

Making use of (A.4), (A.5), (A.6), (A.7), (A.8), (A.9), (A.10), (A.11), (A.12), (A.13), (A.14), and (A.15), the evaluation of the FIM now requires *numerical* averaging over $\tilde{\mathbf{z}}$ only. This reduces the numerical complexity considerably.

Note from (A.6), (A.7), (A.10), (A.11), (A.12), and (A.13) that $J_{\theta,F}$, $J_{F,F}$, and $J_{F,\tau}$ are functions of the parameter τ. This implies that the CRB depends on the exact value of the unknown but deterministic time delay $\tau \in [-T/2, T/2]$ that is being estimated. However, under the usual assumption that the observation interval is much longer than the symbol duration ($L \gg 1$), this dependence can be safely ignored, because we can use in (A.6), (A.7), (A.10), (A.11), (A.12), and (A.13) the approximations $kT+\tau \cong kT$ and $k'T+\tau \cong k'T$ when summing over k and k' in (17). A similar reasoning was made in [3] regarding the computation of the MCRB. Numerical results for different values of τ (not reported here) confirm this behavior.

ACKNOWLEDGMENT

This work was supported by the Interuniversity Attraction Poles Program P5/11, Belgian Science Policy.

REFERENCES

[1] H. L. Van Trees, *Detection, Estimation and Modulation Theory*, Wiley, New York, NY, USA, 1968.

[2] A. N. D'Andrea, U. Mengali, and R. Reggiannini, "The modified Cramer-Rao bound and its application to synchronization problems ," *IEEE Trans. Commun.*, vol. 42, no. 234, pp. 1391–1399, 1994.

[3] F. Gini, R. Reggiannini, and U. Mengali, "The modified Cramer-Rao bound in vector parameter estimation," *IEEE Trans. Commun.*, vol. 46, no. 1, pp. 52–60, 1998.

[4] W. G. Cowley, "Phase and frequency estimation for PSK packets: bounds and algorithms," *IEEE Trans. Commun.*, vol. 44, no. 1, pp. 26–28, 1996.

[5] F. Rice, B. Cowley, B. Moran, and M. Rice, "Cramer-Rao lower bounds for QAM phase and frequency estimation," *IEEE Trans. Commun.*, vol. 49, no. 9, pp. 1582–1591, 2001.

[6] N. Noels, H. Steendam, and M. Moeneclaey, "The true Cramer-Rao bound for carrier frequency estimation from a PSK signal," *IEEE Trans. Commun.*, vol. 52, no. 5, pp. 834–844, 2004.

[7] N. Noels, H. Wymeersch, H. Steendam, and M. Moeneclaey, "True Cramer-Rao bound for timing recovery from a bandlimited linearly Modulated waveform with unknown carrier phase and frequency ," *IEEE Trans. Commun.*, vol. 52, no. 3, pp. 473–483, 2004.

[8] N. Noels, H. Steendam, and M. Moeneclaey, "The Cramer-Rao bound for phase estimation from coded linearly modulated signals ," *IEEE Commun. Lett.*, vol. 7, no. 5, pp. 207–209, 2003.

[9] N. Noels, C. Herzet, A. Dejonghe, et al., "Turbo synchronization: an EM algorithm interpretation ," in *Proc. IEEE International Conference on Communications (ICC '03)*, vol. 4, pp. 2933–2937, Anchorage, AK, USA, May 2003.

[10] M. Moeneclaey, "On the true and the modified Cramer-Rao bounds for the estimation of a scalar parameter in the presence of nuisance parameters," *IEEE Trans. Commun.*, vol. 46, no. 11, pp. 1536–1544, 1998.

[11] L. Bahl, J. Cocke, F. Jelinek, and J. Raviv, "Optimal decoding of linear codes for minimizing symbol error rate," *IEEE Trans. Inform. Theory*, vol. 20, no. 2, pp. 248–287, 1974.

[12] C. Berrou and A. Glavieux, "Near optimum error correcting coding and decoding: turbo-codes," *IEEE Trans. Commun.*, vol. 44, no. 10, pp. 1261–1271, 1996.
[13] T. Richardson, "The geometry of turbo-decoding dynamics ," *IEEE Trans. Inform. Theory*, vol. 46, no. 1, pp. 9–23, 2000.
[14] D. Rife and R. Boorstyn, "Single tone parameter estimation from discrete-time observations ," *IEEE Trans. Inform. Theory*, vol. 20, no. 5, pp. 591–598, 1974.
[15] A. J. Viterbi and A. M. Viterbi, "Nonlinear estimation of PSK-modulated carrier phase with application to burst digital transmission ," *IEEE Trans. Inform. Theory*, vol. 29, no. 4, pp. 543–551, 1983.
[16] A. A. D'Amico, A. N. D'Andrea, and R. Regiannini, "Efficient non-data-aided carrier and clock recovery for satellite DVB at very low signal-to-noise ratios ," *IEEE J. Select. Areas Commun.*, vol. 19, no. 12, pp. 2320–2330, 2001.
[17] R. A. Boyles, "On the convergence of the EM algorithm," *Journal of the Royal Statistical Society: Series B*, vol. 45, no. 1, pp. 47–50, 1983.
[18] B. P. Beahan, "Frequency estimation of partitioned reference symbol sequences," M.S. thesis, University of South Australia, Adelaide, South Australia, Australia, April 2001, http://www.itr.unisa.edu.au/~steven/thesis.
[19] J. A. Gansman, J. V. Krogmeier, and M. P. Fitz, "Single frequency estimation with non-uniform sampling," in *Proc. of the 13th Asilomar Conference on Signals, Systems and Computers*, vol. 1, pp. 399–403, Pacific Grove, CA , USA, November 1996.
[20] H. Wymeersch, N. Noels, H. Steendam, and M. Moeneclaey, "Synchronization at low SNR: performance bounds and algorithms," in *IEEE Communication Theory Workshop (CTW '04)*, Capri, Italy, May 2004.
[21] C. Herzet, V. Ramon, L. Vandendorpe, and M. Moeneclaey, "Em algorithm-based timing synchronization in turbo receivers," in *IEEE International Conference on Acoustics, Speech and Signal Processing (ICASSP '03)*, vol. 4, pp. 612–615, Hong Kong, China, April 2003.

N. Noels received the Diploma of Electrical Engineering from Ghent University, Ghent, Belgium, in 2001. She is currently a Ph.D. Student at the Department of Telecommunications and Information Processing, Ghent University. Her main research interests are in carrier and symbol synchronization. She is the author of several papers in international journals and conference proceedings.

H. Steendam received the Diploma of Electrical Engineering and the Ph.D. degree in electrical engineering from Ghent University, Ghent, Belgium, in 1995 and 2000, respectively. She is a Professor at the Department of Telecommunications and Information Processing, Ghent University. Her main research interests are in statistical communication theory, carrier and symbol synchronization, bandwidth-efficient modulation and coding, spread spectrum (multicarrier spread spectrum), and satellite and mobile communication. She is the author of more than 50 scientific papers in international journals and conference proceedings.

M. Moeneclaey received the Diploma and the Ph.D. degree, both in electrical engineering, from Ghent University, Ghent, Belgium, in 1978 and 1983, respectively. He is currently a Professor at the Department of Telecommunications and Information Processing, Ghent University. His main research interests are in statistical communication theory, carrier and symbol synchronization, bandwidth-efficient modulation and coding, spread spectrum, and satellite and mobile communication. He is the author of about 250 scientific papers in international journals and conference proceedings. Together with H. Meyr (RWTH Aachen) and S. Fechtel (Siemens AG), he is the coauthor of the book *Digital Communication Receivers–Synchronization, Channel estimation, and Signal Processing* (Wiley, New York, 1998).